Polydatin reverses oxidation low lipoprotein (oxLDL)-induced apoptosis of human umbilical vein endothelial cells *via* regulating the miR-26a-5p/BID axis

Dajie Wang,[1#] Zhaofeng Zhou,[1#] Liang Yuan[2]

[1]Department of Cardiology, the Yancheng School of Clinical Medicine of Nanjing Medical University (Yancheng Third People's Hospital), Yancheng, Jiangsu
[2]Department of Cardiology, First Affiliated Hospital of Nanjing Medical University, Nanjing, Jiangsu, China
[#]These authors contributed equally to this work and should be considered as co-first authors

ABSTRACT

Atherosclerosis is a disease in which lipids and inflammatory factors accumulate on the walls of arteries, forming plaques that eventually block the flow of blood. Polydatin was derived from plant knotweed, which could play an important role in inhibiting the progression of atherosclerosis. However, the mechanism by which polydatin regulates the genesis and development of atherosclerosis remains unclear. To detect the function of polydatin in atherosclerosis, the proliferation, apoptosis and migration of human umbilical vein endothelial cells (HUVECs) was detected using 5-ethynyl-2'-deoxyuridine staining, flow cytometry and transwell assays, respectively. In addition, the branch points and capillary length of HUVECs were observed using a tube formation assay, and the lipid accumulation was tested by Oil-red O staining assay. Dual luciferase reporter assays were performed to confirm the association between microRNA (miR)-26a-5p and BH3 interacting domain death agonist (BID) in HUVECs. The data suggested oxidized low-density lipoprotein (oxLDL) notably inhibited the viability of HUVECs in a dose-dependent manner, and polydatin reversed the oxLDL-induced inhibition of HUVECs viability and proliferation. In addition, polydatin inhibited the apoptosis, migration and epithelial mesenchymal transition (EMT) process in oxLDL-treated HUVECs. Polydatin reversed oxLDL-induced lipid accumulation and angiogenesis inhibition in HUVECs. Furthermore, BID was targeted by miR-26a-5p, and polydatin reversed the oxLDL-induced apoptosis of HUVECs *via* regulating the miR-26a-5p/BID axis. In summary, polydatin reversed the oxLDL-induced apoptosis of HUVECs *via* regulating the miR-26a-5p/BID axis. Therefore, polydatin could act as a new agent for atherosclerosis treatment.

Key words: Atherosclerosis; polydatin; miR-26a-5p; BH3 interacting domain death agonist.

Correspondence: Liang Yuan, Department of Cardiology, First Affiliated Hospital of Nanjing Medical University, 300 Guangzhou Rd, Nanjing, Jiangsu 210029, China

Contributions: DW, LY, experiments design; DW, ZZ, experiments performing; LY, study supervision, manuscript review and revision. All the authors have read and approved the final version of the manuscript and agreed to be accountable for all aspects of the work.

Conflict of interest: The authors declare that they have no competing interests, and all authors confirm accuracy.

Ethical approval: No Ethical Committee approval was required for this study, as it does not contain any studies with human participants or animals.

Availability of data and materials: The datasets used and/or analyzed during the current study are available from the corresponding author on reasonable request.

Introduction

Atherosclerosis is a disease in which substances (such as lipids and inflammatory factors) accumulate on the walls of arteries, forming plaques that narrow and harden the blood vessels, and eventually block the flow of blood,[1,2] It is hypothesized that atherosclerosis is associated with injury of vascular endothelial cells and chronic inflammation.[3] Vascular endothelial cells are flat cells that cover the lumen surface of blood vessels.[3] Maintaining the integrity of the structure and physiological functions of such cells can effectively control the development of atherosclerosis.[4] However, the pathogenesis of atherosclerosis is currently unclear.[5] The main risk factors for the occurrence and development of atherosclerosis include dyslipidemia, increased blood pressure and obesity.[6] At present, the therapeutic measures for atherosclerosis are interventional therapy, drug therapy and surgery.[7,8] However, the results of these treatments remain unsatisfactory.

Polydatin is a natural active ingredient from *Rhizoma Polygoni Cuspidati*, which is a traditional Chinese medicine.[9,10] It has been reported that polydatin has anti-inflammatory and anti-apoptotic effects in a variety of cardiovascular diseases such as atherosclerosis.[9,11,12] Peng *et al.*[11] reported that polydatin could inhibit the progression of atherosclerosis by reducing macrophage infiltration and the expression of inflammatory factors. In addition, Huang *et al.*[13] indicated that polydatin is remarkably effective in inhibiting the progression of atherosclerosis. However, the mechanism by which polydatin regulates the genesis and development of atherosclerosis remains unclear.

MicroRNAs (miRNAs) are RNA molecules 21-23 nucleotides in length, which are present in eukaryotes.[13,14] MiRNAs can inhibit the expression of post-transcriptional genes by specifically binding to target mRNA, and play an important role in regulating the cell cycle and gene expression.[13,14]. miRNAs have been the focus of numerous studies as potential biomarkers or therapeutic targets.[15-17]. Specifically, miRNAs are associated with the proliferation of vascular endothelial cells.[17,18] For example, the increase in miR-342-5p significantly promoted the apoptosis of human umbilical vein endothelial cells (HUVECs) treated with H_2O_2.[17] In addition, miR-485-3p is closely associated with the proliferation of human microvascular endothelial cells cultured under hypoxic conditions.[19] Furthermore, miR-26a-5p was significantly downregulated in primary endothelial cells from CAD mice.[18]

Based on the above background, the present study aimed to explore the association between polydatin, miR-26a-5p and atherosclerosis. We hope this study might provide new strategies for clinicians to treat atherosclerosis.

Materials and Methods

Cell culture

HUVECs were from American Type Culture Collection and maintained in DMEM (Thermo Fisher Scientific, Inc., Waltham, MA, USA) containing 1% penicillin and streptomycin at 37°C in a humidified atmosphere with 5% CO_2.

5-Ethynyl-2'-deoxyuridine (EdU) staining

The EdU detection kit was obtained from Guangzhou RiboBio Co., Ltd (Guangzhou, China). Firstly, HUVECs were cultured to the logarithmic growth stage and then incubated with 50 μM EdU (Beyotime Institute of Bioechnology, Haimen, China; 100 μL). Next, the medium was removed, and the cells were washed with PBS twice for 5 min each time. HUVECs were then incubated with 1 μg/mL DAPI (Beyotime Institute of Bioechnology; 100 μL) in the dark. Finally, the cells were observed using a fluorescence microscope (CX23, Olympus Co., Shinjuku, Tokyo, Japan; three microscope fields were considered). Three replicates were performed in each group.

Flow cytometry assay

Firstly, HUVECs were digested with 0.25% trypsin, and then collected by centrifugation at room temperature at 2,000 rpm for 10 min. Next, cells were incubated with 5 μL annexin V (3%; BD Bioscience, Franklin Lakes, NJ, USA), followed by incubation with 5 μL propidium iodide (3%; BD Bioscience) for 15 min in the dark. Finally, HUVECs undergoing apoptosis (early + late) were detected by flow cytometry (Accuri C6; BD Biosciences) and cell apoptosis was determined using FlowJo 7.6.1 software (FlowJo LLC, Ashland, OR, USA). Three replicates were performed in each group.

Transwell assay

HUVECs were added to the upper chamber of the transwell insert, which contained 200 μL serum-free medium, while the lower chamber contained 600 μL DMEM with 10% FBS. The HUVECs that had migrated to the lower membrane surface were stained with crystal violet (0.1%) for 10 min after 24 h of incubation. Finally, the migrated cells were observed using a light microscope (BX53, Olympus Co).

Western blotting

Protein Lysis Buffer (Beyotime Institute of Biotechnology) was used to isolate total protein from HUVECs. The protein concentration was quantified with a BCA protein assay kit (Beyotime Institute of Biotechnology). Next, proteins were separated using 10% SDS-PAGE and transferred to PVDF membranes, which were then blocked with 3% skimmed milk, followed by incubation overnight at 4°C with primary antibodies (anti-E-cadherin: 1:1,000; anti-N-cadherin: 1:1,000; anti-vimentin: 1:1,000; anti-BID: 1:1,000; anti-cleaved caspase 3: 1:1,000; anti-β-actin: 1:1,000) and subsequent incubation with a horseradish peroxidase-conjugated goat anti-rabbit IgG polyclonal secondary antibody (1:5,000) for 1 h at room temperature. All antibodies were purchased from Abcam (Cambridge, UK). Next, the membranes were subjected to enhanced chemiluminescence using a kit. β-actin was used as an internal loading control for normalization.

Tube formation assay

Matrigel™ (BD Biosciences) was used to detect the tube formation of HUVECs. A total of 5×10^4 HUVECs were plated on a 96-well plate precoated with Matrigel™ (50 μL/well) for 30 min at 37°C. After 12 h, the enclosed networks of tubes from six random high-power microscope fields were examined under a light microscope (BX53, Olympus). The mean value of 10 cumulative total lengths per well represented an experimental point. The number of tubes was assessed using ImageJ 1.52 k software (version 1.46; National Institutes of Health). Three replicates were performed in each group.

Oil-red-O staining assay

Oil-red-O staining was performed to observe lipid accumulation in HUVECs. Cells were fixed with 10% paraformaldehyde for 30 min and then stained with Oil-red O (30%; Beyotime Institute of Biotechnology) for 10 min, followed by sealing the coverslip with glycerin gelatin. Subsequently, Oil-red-O staining was observed using a light microscope (BX53, Olympus Co.). Three replicates were performed in each group. Six random high-power microscope fields were performed.

RT-qPCR

TRIzol® reagent (ELK Biotechnology, Co., Ltd., Wuhan, China)

was used to extract total RNA from HUVECs, and an EntiLink™ 1st strand cDNA Synthesis Kit (ELK Biotechnology, Co., Ltd.) was then used to synthesize cDNA. Next, RT-qPCR was performed on a StepOne™ Real-Time PCR System. The 2^{-DDCq} method was used to quantify the data. The primers used in the present study were purchased from Shanghai GenePharma Co., Ltd. (Shanghai, China), and their sequences are as follows: U6 forward, 5'-CTCGCTTCGGCAGCACA-3', reverse, 5'-AACGCTTCACGAATTTGCGT-3'; β-actin forward, 5'-GTCCACCGCAAATGCTTCTA-3', reverse, 5'-TGCTGTCACCTTCACCGTTC-3'; miR-342-5p, 5'-AGGGGTGCTATCTGTGATTGA-3'; miR-485-3p forward, 5'-GGCCGTCATACACGGCTC-3', reverse, 5'-CTCAACTGGTGTCGTGGAGTC-3'; miR-26a-5p forward, 5'-UCCAUAAAGUAGGAAACACUACA-3', reverse, 5'-CAGUACUUUUGUGUAGUACAA-3'; and BID forward, 5'-AAGAAGGTGGCCAGTCACAC-3', reverse, 5'-GTCCATCCCATTTCTGGCTA-3'.

Cell transfection

MiR-26a-5p mimics, miR-26a-5p mimics-control (ctrl), pcDNA3.1-overexpression (OE)-ctrl and pcDNA3.1-BID OE were obtained from Shanghai GenePharma Co., Ltd., and were transfected into HUVECs using Lipofectamine® 2000 (Invitrogen, Waltham, MA, USA) according to the manufacturer's protocol.

Dual luciferase reporter assay

Wild-type (WT) and mutated (MT) reporter vectors for miR-26a-5p and BID were constructed by Sangon Biotech Co., Ltd. (Shanghai, China). BID WT or BID MT together with miR-26a-5p mimics or miR-26a-5p mimics-ctrl were transfected into HUVECs using Lipofectamine® 2000 (Invitrogen) according to the manufacturer's protocol. Subsequently, luciferase activity in HUVECs was detected using a Dual Luciferase Reporter Assay System (Beyotime Institute of Biotechnology).

Statistical analysis

The experiments were repeated three times, and the data are presented as the mean ± SD. Comparisons between ≥3 groups were analyzed using a one-way ANOVA followed by a Tukey's *post-hoc* test. A p-value <0.05 was considered to indicate a statistically significant difference.

Results

Polydatin reverses the oxLDL-induced inhibition of HUVEC viability and proliferation

In order to mimic atherosclerosis *in vitro*, HUVECs were treated with oxLDL. As indicated in Figure 1A, oxLDL (0, 30, 60 and 120 μg/mL) notably inhibited the viability of HUVECs in a dose-dependent manner. Since 60 μg/mL oxLDL exerted a mild cytotoxicity in HUVECs, while 120 μg/ml oxLDL exerted a high cytotoxicity in HUVECs, 60 μg/mL oxLDL was selected for subsequent

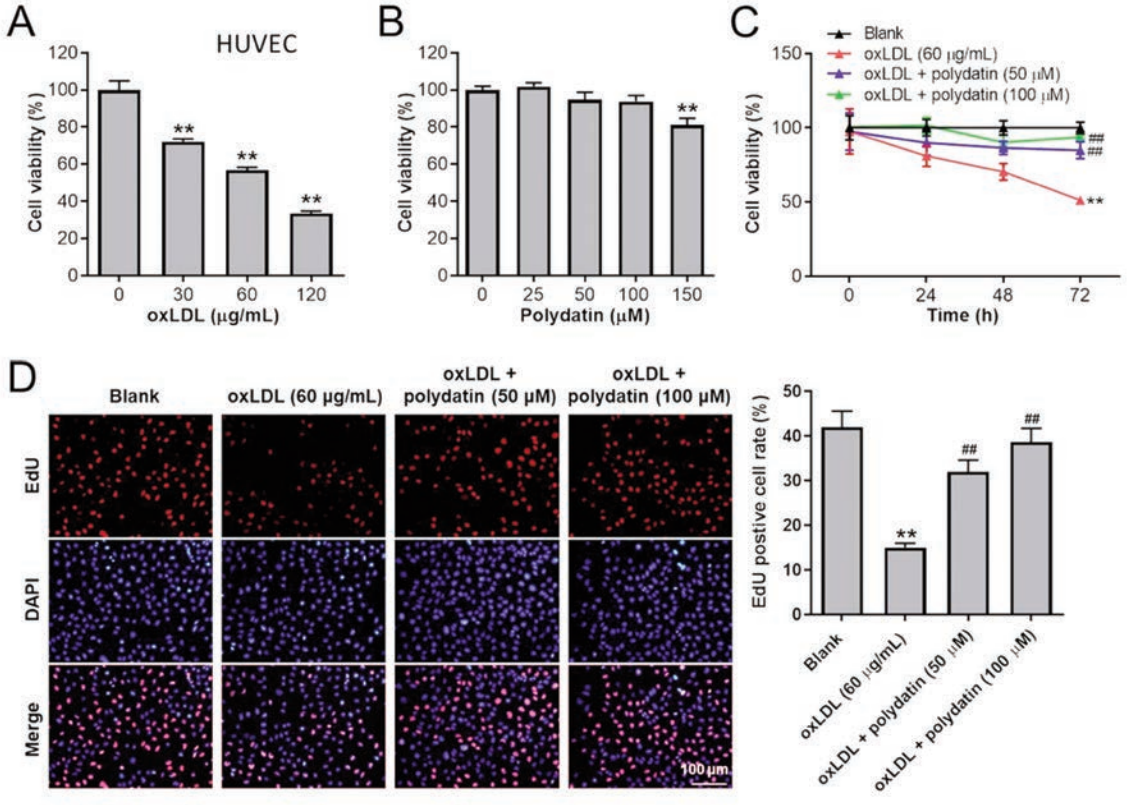

Figure 1. Polydatin reverses oxLDL-induced inhibition of HUVECs viability and proliferation. A) Different concentrations of oxLDL (0, 30, 60 and 120 g/mL) were used to treat HUVECs. B) Different concentrations of polydatin (0, 25, 50, 100 and 150 M) were used to treat HUVECs. C) OxLDL (60 g/mL) and polydatin (50 or 100 M) were used to treat HUVECs. The viability of HUVECs was measured by CCK8 assay. D) The proliferation of HUVECs was measured by EdU assay. Three replicates were performed in each group. **p<0.01 compared with control group; ##p<0.01 compared with oxLDL (60 g/mL) treated group.

analyses (Figure 1A). Polydatin dose dependently inhibited the viability of HUVECs (Figure 1B). Since 50 and 100 μM polydatin showed minimal cytotoxicity towards the viability of HUVECs, and 150 μM polydatin had a strong toxic effect on the viability of HUVECs, 50 or 100 μM polydatin was selected for subsequent experiments (Figure 1B). OxLDL markedly inhibited the viability of HUVECs, compared with that of the control group, while this phenomenon was notably reversed by polydatin (Figure 1C). Consistently, oxLDL significantly inhibited the proliferation of HUVECs, while this phenomenon was abolished by polydatin (Figure 1D). Collectively, polydatin could reverse the oxLDL-induced inhibition of HUVEC viability and proliferation.

Polydatin reverses oxLDL-induced apoptosis, migration and epithelial-mesenchymal transition (EMT) in HUVECs

To assess the function of polydatin on HUVECs apoptosis, flow cytometry was employed. OxLDL notably induced the apoptosis of HUVECs, while the pro-apoptotic effect of oxLDL was markedly inhibited by polydatin (Figure 2A). In addition, oxLDL significantly promoted the migration of HUVECs, and this phenomenon was mainly reversed in the presence of polydatin (Figure 2B). As expected, oxLDL notably downregulated the level of E-cadherin, and upregulated the levels of N-cadherin and vimentin in HUVECs, while these effects of oxLDL were significantly reversed by polydatin (Figure 2C). To summarize, polydatin could notably reverse oxLDL-induced apoptosis, migration and EMT in HUVECs.

Polydatin reverses the oxLDL-induced lipid accumulation and angiogenesis inhibition of HUVECs

To investigate the effect of polydatin on HUVEC angiogenesis, a tube formation assay was performed. As revealed in Figure 3A, oxLDL visibly inhibited the angiogenesis of HUVECs, and this phenomenon was reversed by polydatin.

The results of Oil-red-O staining showed that oxLDL remarkably induced lipid accumulation in HUVECs; however, this phenomenon was abolished by polydatin (Figure 3B). In general, polydatin could reverse the oxLDL-induced lipid accumulation and angiogenesis inhibition of HUVECs.

BID is targeted by miR-26a-5p, and polydatin reverses the oxLDL-induced apoptosis of HUVECs *via* regulating the miR-26a-5p/BID axis

To investigate the mechanism by which polydatin regulates the progression of atherosclerosis, various miRNAs were selected in the present study. It has been reported that miR-342-5p, miR-485-3p and miR-26a-5p are associated with the proliferation of vascular endothelial cells.[17-19] Therefore, RT-qPCR was performed to detect the expression of these miRNAs. As indicated in Figure 4A, polydatin significantly upregulated the expression of miR-26a-5p in HUVECs, while polydatin had no effect on the levels of miR-342-5p or miR-485-3p. Furthermore, miR-26a-5p plays a crucial role in the development of atherosclerosis.[20] Thus, miR-26a-5p was evaluated in the following experiments. To further study the mechanism by which polydatin and miR-26a-5p regulate the development of

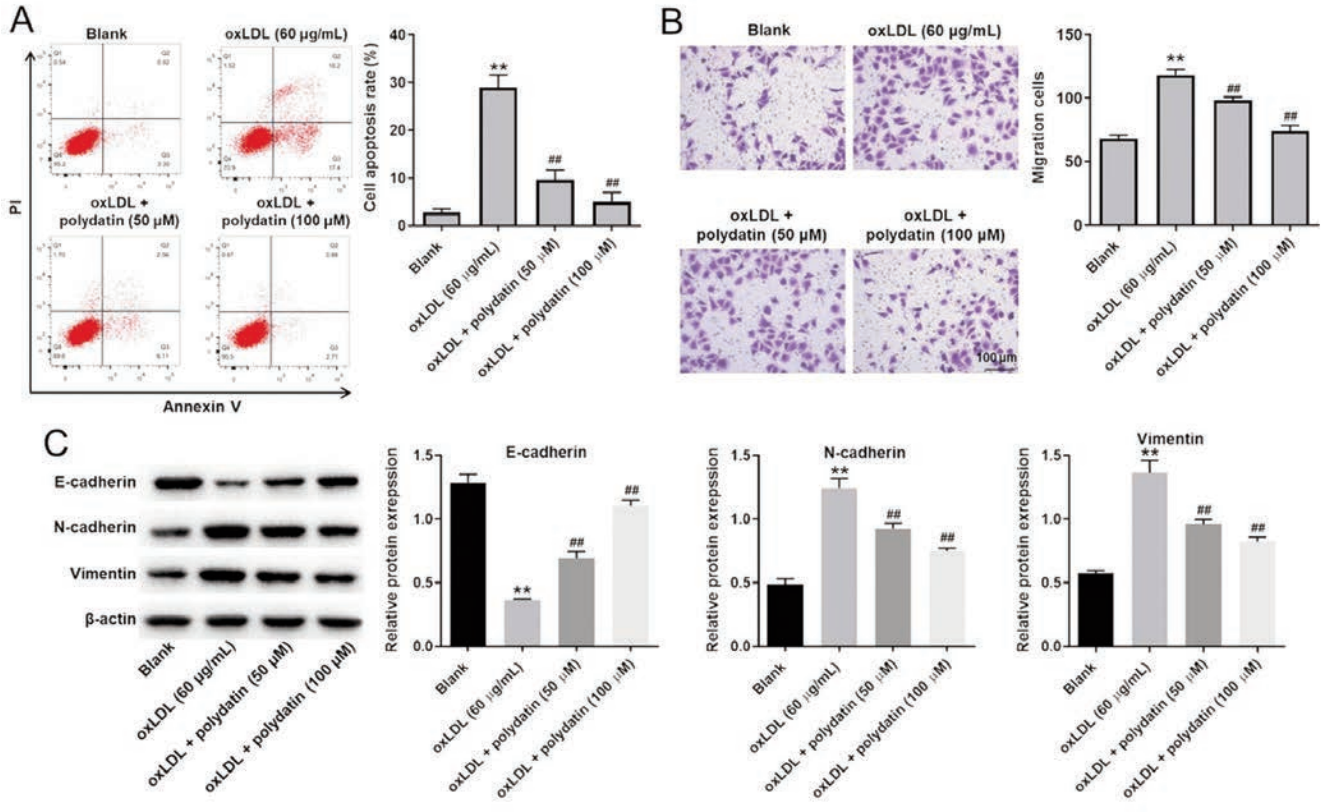

Figure 2. **Polydatin reverses oxLDL-induced apoptosis, migration and EMT process of HUVECs. A) OxLDL (60 μg/mL) and polydatin (50 or 100 μM) were used to treat HUVECs. The apoptosis of HUVECs was measured using flow cytometry. B) The migration of HUVECs was detected using transwell assay. C) The expression levels of E-cadherin, N-cadherin and Vimentin were measured by Western blot. Three replicates were performed in each group. **p<0.01 compared with control group; ##p<0.01 compared with oxLDL (60 μg/mL) treated group.**

atherosclerosis, TargetScan and miRDB bioinformatics databases were used in the current study. As suggested in Figure 4B, BID may be a potential direct target of miR-26a-5p, and BID has been reported to play an important role in atherosclerosis.[21] In addition, miR-26a-5p mimics markedly promoted the expression of miR-26a-5p (Figure 4C). miR-26a-5p mimics significantly decreased the luciferase activity of BID-WT in HUVECs; however, the luciferase activity of BID-MT was not affected (Figure 4D).

Consistent with the above data, oxLDL markedly upregulated the expression of BID and cleaved caspase 3; however, these phenomena were abolished in the presence of polydatin (Figure 4 E-G). These data confirmed that BID was targeted by miR-26a-5p and that polydatin could markedly reverse the oxLDL-induced apoptosis of HUVECs *via* regulating the miR-26a-5p/BID axis.

Polydatin reverses the oxLDL-induced inhibition of HUVECs proliferation by regulating the miR-26a-5p/BID axis

To further investigate the mechanism by which the miR-26a-5p/BID axis regulates atherosclerosis, rescue experiments were performed. BID OE markedly increased the level of BID in HUVECs, compared with that of the control group (Figure 5A). In addition, oxLDL significantly induced the apoptosis of HUVECs, while this phenomenon was markedly reversed by polydatin; however, the inhibitory effect of polydatin was abolished by BID OE (Figure 5B). As expected, oxLDL notably inhibited the proliferation of HUVECs, and this inhibition was reversed by polydatin, while the effect of polydatin was abolished in the presence of BID OE (Figure 5C). Taken together, polydatin could notably reverse the oxLDL-induced inhibition of HUVEC proliferation by regulating the miR-26a-5p/BID axis.

Polydatin reverses the oxLDL-induced apoptosis of HUVECs *via* regulation of a miR-26a-5p/BID axis

To further assess the effect of BID OE on apoptosis-related proteins, western blotting was performed. The results indicated that oxLDL notably increased the expression of BID and cleaved caspase 3, while these phenomena were abolished by polydatin. However, the inhibitory effects of polydatin on BID and cleaved caspase 3 were reversed by BID OE (Figure 5 A-C). In summary, polydatin could reverse the oxLDL-induced apoptosis of HUVECs *via* regulation of a miR-26a-5p/BID axis (Figure 6).

Discussion

It has been reported that atherosclerosis is the main cause of myocardial and cerebral infarction.[22,23] On the other hand, polydatin was confirmed to exert anti-inflammatory effect on multiple diseases.[24,25] In this research, polydatin was able to reverse oxLDL-induced HUVEC apoptosis, and it could regulate miR-26a-5p/BID

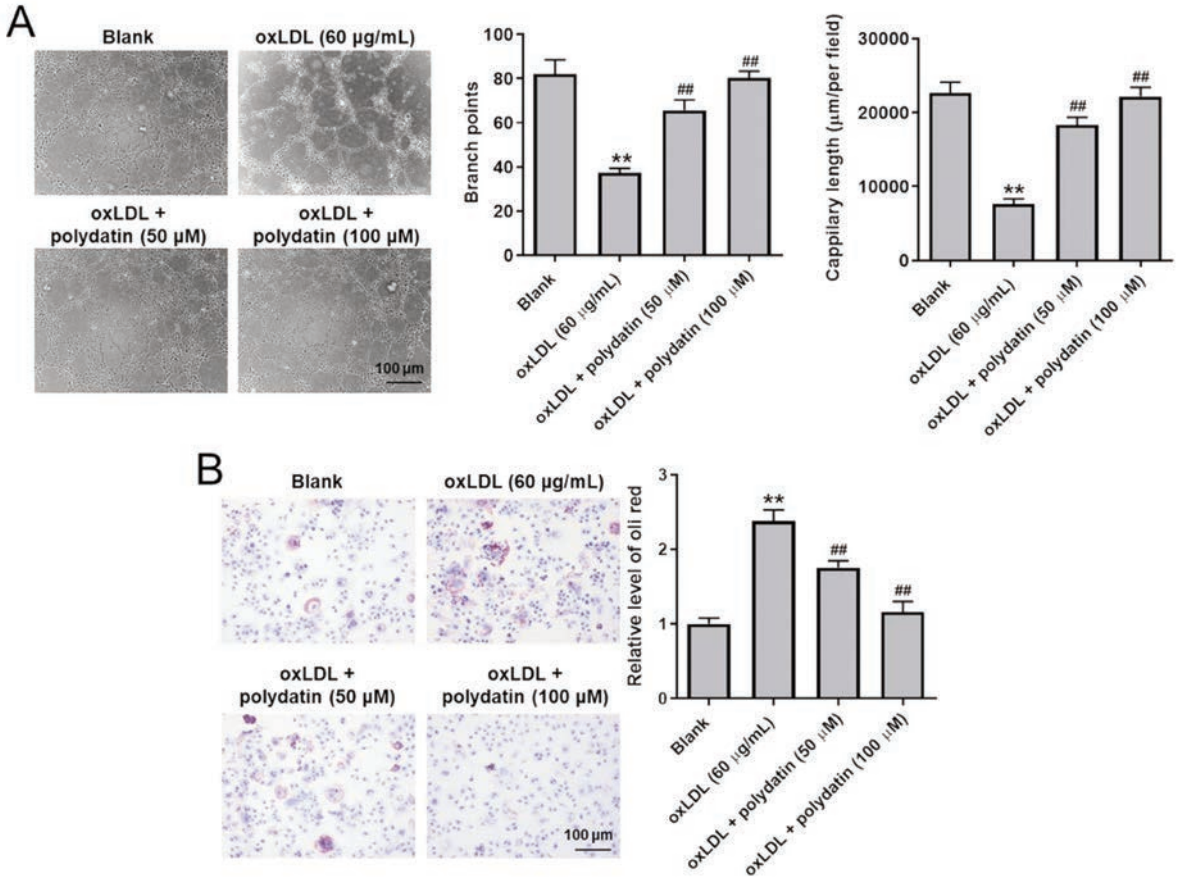

Figure 3. Polydatin reverses oxLDL-induced lipid accumulation and angiogenesis inhibition of HUVECs. A) OxLDL (60 μg/mL) and polydatin (50 or 100 μM) were used to treat HUVECs. The angiogenesis of HUVECs was detected using tube formation assay. B) The lipid accumulation of HUVECs was observed by Oil-red-O staining. Three replicates were performed in each group. **p<0.01 compared with control group; ##p<0.01 compared with oxLDL (60 μg/mL) treated group.

axis. Thus, the present study first explored the mechanism underlying the function of polydatin in oxLDL-treated HUVECs, suggesting that polydatin could serve as a new suppressor in atherosclerosis.

Polydatin is a traditional Chinese medicine that can be used to treat atherosclerosis.[9,10] Gugliandolo *et al.*[26] reported that polydatin could protect vascular cells against IL-1β-induced inflammation and oxidative stress, while Xiong *et al.*[27] indicated that polydatin could significantly inhibit the progression of atherosclerosis. In the present study, polydatin proved to reverse the oxLDL-induced apoptosis, migration and EMT process of HUVECs. miR-26a-5p is closely associated with atherosclerosis.[28,29] Atorvastatin, which is a drug prescribed for the treatment of atherosclerosis, could inhibit the oxLDL-induced apoptosis of HUVECs by regulating the miR-26a-5p/PTEN axis.[28] Kaempferol, which belongs to the family of flavanols, can alleviate the oxLDL-induced apoptosis of HUVECs by upregulating the expression of miR-26a-5p.[28] In the present study, polydatin markedly reversed the oxLDL-induced apoptosis of HUVECs *via* regulation of the miR-26a-5p/BID axis, which was consistent with previous reports.

BID was reported as a crucial mediator in cell growth.[30,31] In addition, BID could act as a promoter in cell apoptosis.[32] In this study, BID was found to be the downstream target of miR-26a-5p. Thus, it might be suggested that polydatin could reverse oxLDL-induced HUVEC injury through regulation of BID. Meanwhile, Xing *et al.* found that miR-26a-5p could inhibit the injury of cardiomyocytes through mediation of PTEN/PI3K/Akt signaling,[33] and our research was similar to this previous research. PTEN was able to inhibit the cell growth through negative regulating Akt signaling,[34] and BID was confirmed to be the pro-apoptotic member. Thus, the similar function between PTEN and BID might contribute to the similarity between our research and the one by Xing *et al.*[33]

The most significant novelty of our study is that for the first time we demonstrated the relationship between polydatin and miR-26a-5p and elucidated its target mRNA in atherosclerosis. Indeed, our research has some limitations: namely, other potential targets of miR-26a-5p are to be further detected, and more downstream miRNAs of polydatin remain unexplored. Hence, further investigations are essential in coming future. In summary, the present findings revealed that polydatin reversed the oxLDL-induced apoptosis of HUVECs *via* regulating the miR-26a-5p/BID axis. Thus, our study might provide a new theoretical basis for exploring new strategies against atherosclerosis.

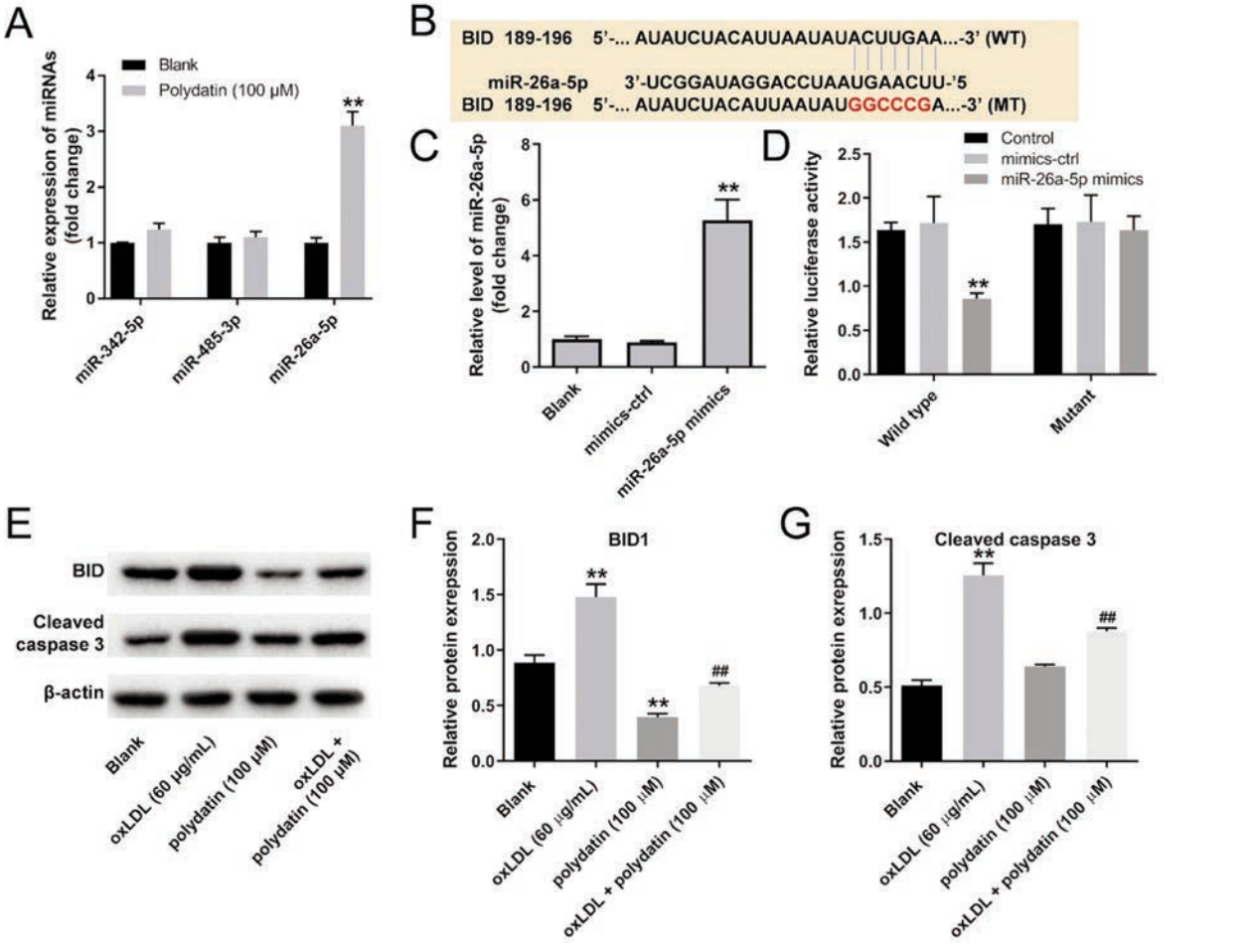

Figure 4. BID is targeted by miR-26a-5p and polydatin reverses oxLDL-induced apoptosis of HUVECs *via* regulating the miR-26a-5p/BID axis. A) The expressions of miR-342-5p, miR-485-3p and miR-26a-5p in HUVECs were measured using RT-qPCR. B) TargetScan and miRDB bioinformatics databases were used to predict the downstream target of miR-26a-5p. C) HUVECs were treated with miR-26a-5p mimics-ctrl or miR-26a-5p mimics; the level of miR-26a-5p was measured using RT-qPCR. D) The luciferase activity of HUVECs that were co-transfected with BID-WT/MT 3'-UTR plasmid and miR-26a-5p mimics was detected using dual luciferase reporter assay. E,F,G) The expression levels of BID and Cleaved caspase 3 were measured by Western blot. Three replicates were performed in each group. **p<0.01 compared with control group; ##p<0.01 compared with oxLDL (60 μg/mL) treated group.

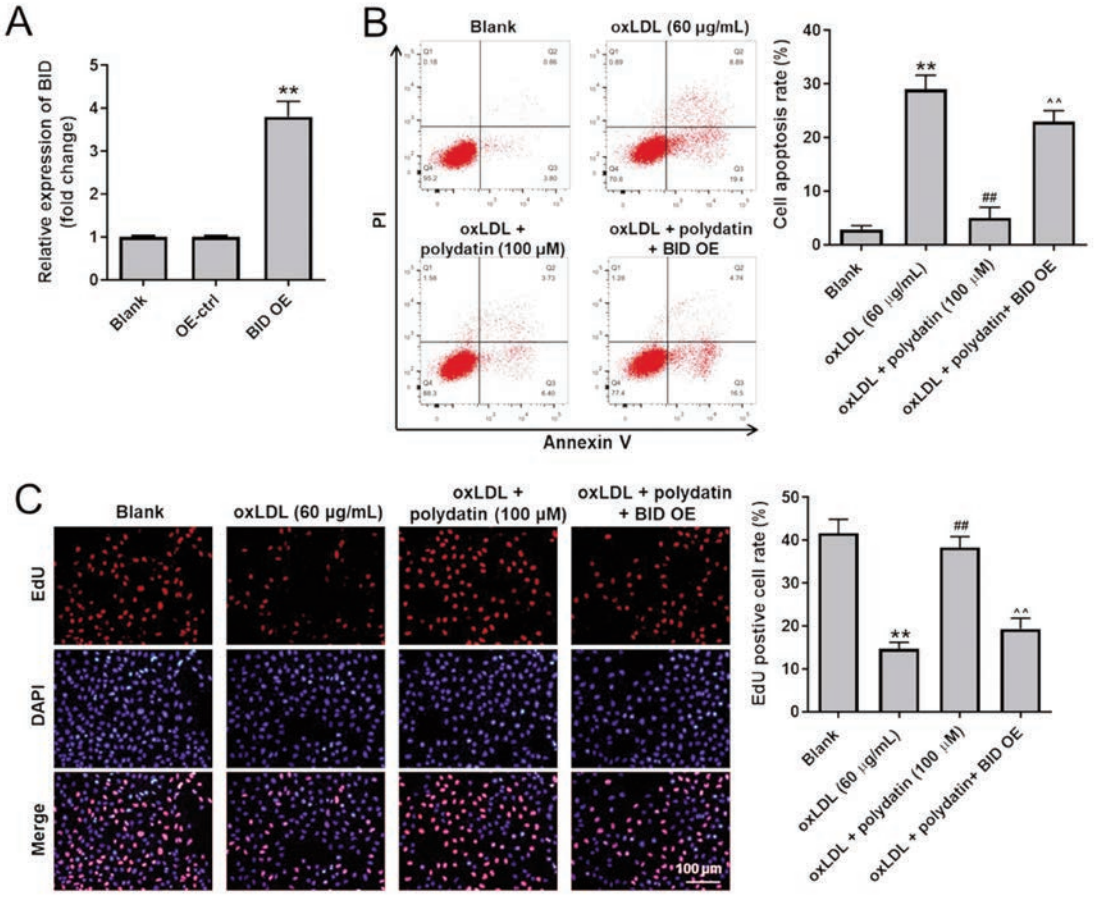

Figure 5. Polydatin reverses oxLDL-induced inhibition of HUVECs proliferation by regulating the miR-26a-5p/BID axis. A) HUVECs were treated with BID OE-ctrl or BID OE. The level of BID was measured using RT-qPCR. B) The apoptosis of HUVECs was measured using flow cytometry. C) The proliferation of HUVECs was measured by EdU assay. Three replicates were performed in each group. **p<0.01 compared with control group; ##p<0.01 compared with oxLDL (60 μg/mL) treated group; ^^p<0.01 compared with oxLDL + polydatin (100 μM) treated group.

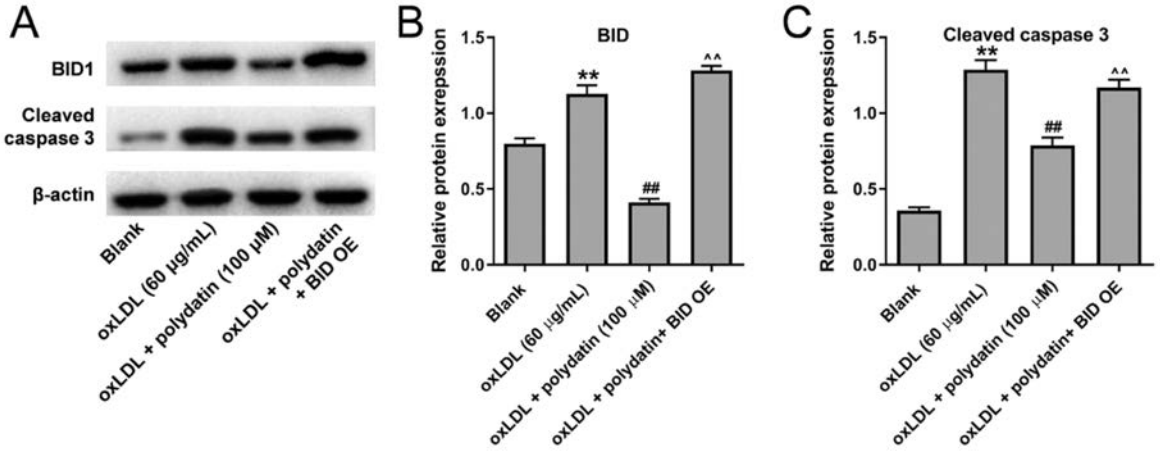

Figure 6. Polydatin reverses oxLDL-induced apoptosis of HUVECs *via* regulating the miR-26a-5p/BID axis. A-C) The expression levels of BID and Cleaved caspase 3 were measured by western blot. Three replicates were performed in each group. ##p<0.01 compared with oxLDL (60 μg/mL) treated group; ^^p<0.01 compared with oxLDL + polydatin (100 μM) treated group.

References

1. Bennett MR, Sinha S, Owens GK. Vascular smooth muscle cells in atherosclerosis. Circ Res 2016;118:692-702.
2. Gimbrone MA Jr., García-Cardeña G. Vascular endothelium, hemodynamics, and the pathobiology of atherosclerosis. Cardiovasc Pathol 2013;22:9-15.
3. Gimbrone MA, Jr., García-Cardeña G. Endothelial cell dysfunction and the pathobiology of atherosclerosis. Circ Res 2016;118:620-36.
4. Yang Q, Xu J, Ma Q, Liu Z, Sudhahar V, Cao Y, et al. PRKAA1/AMPKα1-driven glycolysis in endothelial cells exposed to disturbed flow protects against atherosclerosis. Nat Commun 2018;9:4667.
5. Wolf D, Ley K. Immunity and inflammation in atherosclerosis. Circ Res 2019;124:315-27.
6. Santos MG, Pegoraro M, Sandrini F, Macuco EC. Risk factors for the development of atherosclerosis in childhood and adolescence. Arq Bras Cardiol 2008;90:276-83.
7. Libby P, Buring JE, Badimon L, Hansson GK, Deanfield J, Bittencourt MS, et al. Atherosclerosis. Nat Rev Dis Primers 2019;5:56.
8. Dai T, He W, Yao C, Ma X, Ren W, Mai Y, et al. Applications of inorganic nanoparticles in the diagnosis and therapy of atherosclerosis. Biomater Sci 2020;8:3784-99.
9. Wu M, Li X, Wang S, Yang S, Zhao R, Xing Y, et al. Polydatin for treating atherosclerotic diseases: A functional and mechanistic overview. Biomed Pharmacother 2020;128:110308.
10. Wang D, Luo X, Wang M, Zhou K, Xia Z. Selective separation and purification of polydatin by molecularly imprinted polymers from the extract of Polygoni Cuspidati Rhizoma et Radix, rats' plasma and urine. J Chromatogr B Analyt Technol Biomed Life Sci 2020;1156:122307.
11. Peng Y, Xu J, Zeng Y, Chen L, Xu XL. Polydatin attenuates atherosclerosis in apolipoprotein E-deficient mice: Role of reverse cholesterol transport. Phytomedicine 2019;62:152935.
12. Ma Y, Gong X, Mo Y, Wu S. Polydatin inhibits the oxidative stress-induced proliferation of vascular smooth muscle cells by activating the eNOS/SIRT1 pathway. Int J Mol Med 2016;37:1652-60.
13. Chen L, Heikkinen L, Wang C, Yang Y, Sun H, Wong G. Trends in the development of miRNA bioinformatics tools. Brief Bioinform 2019;20:1836-52.
14. Tiwari A, Mukherjee B, Dixit M. MicroRNA key to angiogenesis regulation: MiRNA biology and therapy. Curr Cancer Drug Targets 2018;18:266-77.
15. Fabris L, Ceder Y, Chinnaiyan AM, Jenster GW, Sorensen KD, Tomlins S, et al. The Ptential of MicroRNAs. Eur Urol 2016;70:312-22.
16. Lu Y, Thavarajah T, Gu W, Cai J, Xu Q. Impact of miRNA in Atheosclerosis. Arterioscler Thromb Vasc Biol 2018;38:e159-e70.
17. Xing X, Li Z, Yang X, Li M, Liu C, Pang Y, et al. Adipose-derived mesenchymal stem cells-derived exosome-mediated microRNA-342-5p protects endothelial cells against atherosclerosis. Aging (Albany NY) 2020;12:3880-98.
18. Jing R, Zhong QQ, Long TY, Pan W, Qian ZX. Downregulated miRNA-26a-5p induces the apoptosis of endothelial cells in coronary heart disease by inhibiting PI3K/AKT pathway. Eur Rev Med Pharmacol Sci 2019;23:4940-7.
19. Hu C, Bai X, Liu C, Hu Z. Long noncoding RNA XIST participates hypoxia-induced angiogenesis in human brain microvascular endothelial cells through regulating miR-485/SOX7 axis. Am J Transl Res 2019;11:6487-97.
20. Ren M, Wang T, Han Z, Fu P, Liu Z, Ouyang C. Long noncoding RNA OIP5-AS1 miR-26a-5p Throuh the AKT/NF-κB Patway. J Cardiovasc Pharmacol 2020;76:635-44.
21. Liu Y, Liu N, Liu Q. Constructing a ceRNA-immunoregulatory network associated with the development and prognosis of human atherosclerosis through weighted gene co-expression network analysis. Aging (Albany NY) 2021;13:3080-100.
22. Swirski FK, Nahrendorf M. Leukocyte behavior in atherosclerosis, myocardial infarction, and heart failure. Science 2013;339:161-6.
23. Yamamoto N, Satomi J, Yamamoto Y, Shono K, Kanematsu Y, Izumi Y, et al. Risk factors of neurological deterioration in patients with cerebral infarction due to large-artery atherosclerosis.J Stroke Cerebrovasc Dis 2017;26:1801-6.
24. Ye G, Zhao Y, Zhu J, Zhang Z, Wang Q, Jiang X, et al. Synergistic TLR4-mediated NF-kappaB actiation in ApoE-deficient mice. Evid Based Complement Alternat Med. 2022;2022:3885153.
25. Gao J, Qian J, Ma N, Han J, Cui F, Chen N, et al. Protective effects of polydatin on reproductive injury induced by ionizing radiation. Dose Response 2022;20:15593258221107511.
26. Gugliandolo E, Fusco F, Biundo F, D'Amico R, Benedetto F, Di Paola R, Cuzzocrea S. Palmitoylethanolamide and polydatin combination reduces inflammation and oxidative stress in vascular injury. Pharmacol Res 2017;123:83-92.
27. Xiong Q, Yan Z, Liang J, Yuan J, Chen X, Zhou L, et al. Polydatin alleviates high-fat diet induced atherosclerosis in apolipoprotein E-deficient mice by autophagic restoration. Phytomedicine 2021;81:153301.
28. Jia Z, An L, Lu Y, Xu C, Wang S, Wang J, et al. Oxidized (HUVECs) was P miR-26a-5p/phosphatase and tensin homolog (PTEN). Med Sci Monit 2019;25:9836-43.
29. Zhong X, Zhang L, Li Y, Li P, Li J, Cheng G. Kaempferol alleviates ox-LDL-induced apoptosis by up-regulation of miR-26a-5p via inhibiting TLR4/NF-κB pathway in human endothelial cells. Biomed Pharmacother 2018;108:1783-9.
30. Geisslinger F, Muller M, Chao YK, Grimm C, Vollmar AM, Bartel K. Targeting TPC2 sensitizes acute lymphoblastic leukemia cells to chemotherapeutics by impairing lysosomal function. Cell Death Dis 2022;13:668.
31. Sun X, Ren R, Yu X, Peng F, Gao X. Application of color Doppler ultrasound combined with magnetic resonance imaging in placenta accreta. Scanning 2022;2022:1050029.
32. Mahib MR, Hosojima S, Kushiyama H, Kinoshita T, Shiroishi T, Suda T, et al. Caspase-7 mediates caspase-1-induced apoptosis independently of Bid. Microbiol Immunol 2020;64:143-52.
33. Xing X, Guo S, Zhang G, Liu Y, Bi S, Wang X, et al. miR-26a-5p protects against myocardial ischemia/reperfusion injury by regulating the PTEN/PI3K/AKT signaling pathway. Braz J Med Biol Res 2020;53:e9106.
34. Chen CY, Chen J, He L, Stiles BL. PTEN: Tumor suppressor and metabolic regulator. Front Endocrinol (Lausanne) 2018;9:338.

Received for publication: 27 July 2022. Accepted for publication: 9 August 2022.

Licensee PAGEPress, Italy
European Journal of Histochemistry 2022; 66:3505
doi:10.4081/ejh.2022.3505